Multi-camera digital holographic PIV: Tomographic DHPIV

C. H. Atkinson[1] and J. Soria[1]

[1]Laboratory for Turbulence Research in Aerospace and Combustion,
Department of Mechanical Engineering, Monash University,
Victoria, 3800, AUSTRALIA

Abstract

The wide scale application of digital holographic particle image velocimetry (DHPIV) as a three-component three-dimensional (3C-3D) velocity field measurement tool is current restricted by the limited size and resolution of commercially available CCD arrays, resulting in a elongation of particle is the direction normal to the hologram plane. This elongation can be over an order of magnitude greater than the true particle diameter and posses significant problems for the cross-correlation analysis used in particle image velocimetry (PIV). In this paper we discuss a multi-camera method of tomographic digital holographic particle image velocimetry (Tomo-DHPIV) to reconstruct a 3D intensity field without a loss of resolution in the hologram normal direction. Application of this reconstruction technique is provided along with Monte Carlo simulations of the effects of various operating parameters.

Introduction

The experimental investigation of many flows is limited by an inability to measure their instantaneous three dimensional (3D) structure. This in turn places significant limitations on our understanding of the complex turbulent and unsteady phenomena that are commonly found in geophysical and engineering flows.

Digital holographic particle image velocimetry (DHPIV) offers arguably the best prospect for a standard three-component three-dimensional (3C-3D) velocity field measurement tool. The advantage of DHPIV comes the inherent three-dimensonal nature of holographic recording (4). Since a hologram records the pattern of interference between light scattered from particles and that of a reference wave, information about both the amplitude and phase of scattered light are stored (figure 1a). A hologram can then be used to reconstruct the intensity distribution throughout an entire volume (figure 1b). Each hologram therefore records the entire 3D intensity distribution, as opposed to tomographic technqiues that rely on trying to solve for the 3D intensity distribution based on a multiple 2D images. 3C-3D velocity fields can then be determine from pairs of reconstructed holograms using 3D cross-correlation techniques, similar to that of standard planer PIV (2).

The use of CCD arrays for holographic recording removes the need for time consuming film processing and enables direct digital holographic reconstruction, without the need for complex optical reconstruction and scanning digitization. This provides a significant step towards mainstream use of DHPIV, yet as with the move from film based PIV to digital PIV, does so at the expense of resolution. Unfortunately this loss of recording resolution is far more serious in DHPIV owing to effect of resolution limited interference fringe spacing on the depth-of-field and accuracy normal to the hologram plane (3). In the case of in-line holography of 11 μm diameter spherical particles this accuracy normal to the hologram can be can be on the order of 20 times the particle diameter, resulting in the reconstruction of ellipsoids in the normal direction. This particle elongation can not only obscure other particles, but can also result in cross-talk between planes normal to the viewing direction, with both effects being highly undesirable in cross-correlation PIV analysis.

In this paper we discuss a new technique of tomographic digital holographic particle image velocimetry (tomo-DHPIV) (6) where multiple holographic reconstructions or 3D projections from different orientations are combined to remove depth-of-field limitations. By retaining only the region of a particles that fall in the overlapping domain of multiple cameras the depth-of-field bias of each view is removed, resulting in a more accurate quasi-spherical particle reconstruction. A discussion of the technique is provided along with a numerical investigation of the optimal operating parameters.
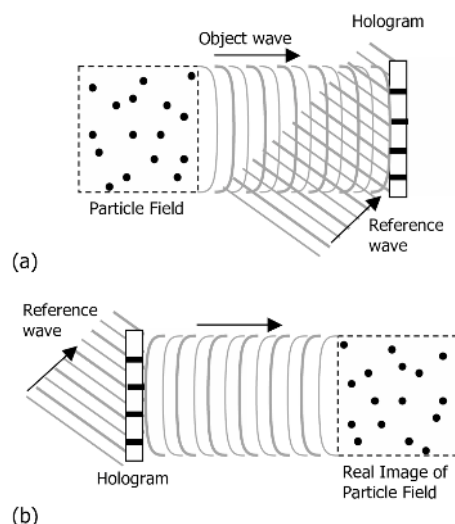

Figure 1: Schematic of (a) holographic recording and (b) holographic reconstruction.

Digital Holography and Depth-of-Field

In digital particle holography the interference pattern created by the light scatter from the particles or the object wave and that of a reference wave is recorderd directly onto a CCD array. These waves may either originate from two separate coherent beams or in the case of in-line holography a single beam where the light scattered by the particles forms the object wave and the light that passes through the particle field forms the reference wave. One advantage of digital holography is that once the interference pattern is recorded it is instantly available in a digital form, without the need to develope and then digitise a holographic plate. The other advantage is that using algorithms such as that of Onural and Scott (5) the 3D volume intensity field may be directly calculated from the digital hologram, replacing the time consuming process of realigning and reprojecting the reference wave through a developed hologram.

During reconstruction the hologram acts in a similar manner to that of a lens, in that it has a finite size and therefore a finite aperture angle. This aperture angle affects the spread of light intensity through the hologram from Fraunhofer diffraction, just as an Airy pattern is created by diffraction through a lens. The intensity spread δ normal to the hologram plane around a reconstructed particle depends on both the diffraction through the hologram and the defocus about the particles true location (4) as:

$$\delta^2(z) = \left(\frac{z-f}{f}D\right)^2 + \left(\frac{2\lambda z}{D}\right)^2 \qquad (1)$$

where z is normal to the hologram plane, f is the distance from the hologram to the particle, D is the hologram aperture or CCD array size and λ is the wavelength of the reconstruction and recording beams. For large f the small angle approximation can be used to express equation 1 in terms of the aperture half angle Ω:

$$\delta^2(z) = 4\Omega^2(z-f)^2 + \left(\frac{\lambda z}{f\Omega}\right)^2 \qquad (2)$$

From this the resolution limit or the smallest particle size parallel to the hologram plane $\Delta_{x,y}$ and that normal to the hologram Δ_z defined as the distance from the front to the rear of the particle where the intensity is halved, can be expressed in terms of the aperture half angle:

$$\Delta_{x,y} = \frac{\lambda}{\Omega} \qquad (3)$$

$$\Delta_z = \frac{\lambda}{\Omega^2} \qquad (4)$$

The largest possible aperture half angle for a given holographic setup is governed by the minimum hologram dimension D or in the case of digital holography the physical size of the CCD array:

$$\Omega = \tan^{-1}\left(\frac{D}{2f}\right) \qquad (5)$$

The effective aperture half angle may however be smaller than this because of the limited resolution of the CCD array. As the interference pattern between the particle object wave and the reference wave spreads towards the edges of the hologram the interference fringes move closer together. With a finite resolution this pattern can only spread so far before it is impossible to distinguish between interference fringes. This represents the resolution limited aperture angle of a digitial hologram (3):

$$\Omega = \tan^{-1}\left(\frac{\lambda}{2\Delta}\right) \qquad (6)$$

where Δ is the CCD pixel size. In the case of in-line holography this angle may be further limited by the Mie scattering when particles are an order of magnitude greater than the scattering wavelength (1). In such cases the scattered light will be predominantly contained in the forward scattering lobe, limiting the interference pattern to an effective half angle based on the particle diameter d:

$$\Omega = \frac{\lambda}{d} \qquad (7)$$

The limited resolution in the scattering direction (equation 4) represents the fundamental draw back in HPIV, the depth-of-field problem. The finite aperture angle limits the resolution that can be obtained in the hologram normal direction and results in the ellipsoid reconstruction of spherical particles. This presents a significant problem for cross-correlation PIV analysis requiring extremely large interrogation windows and vector
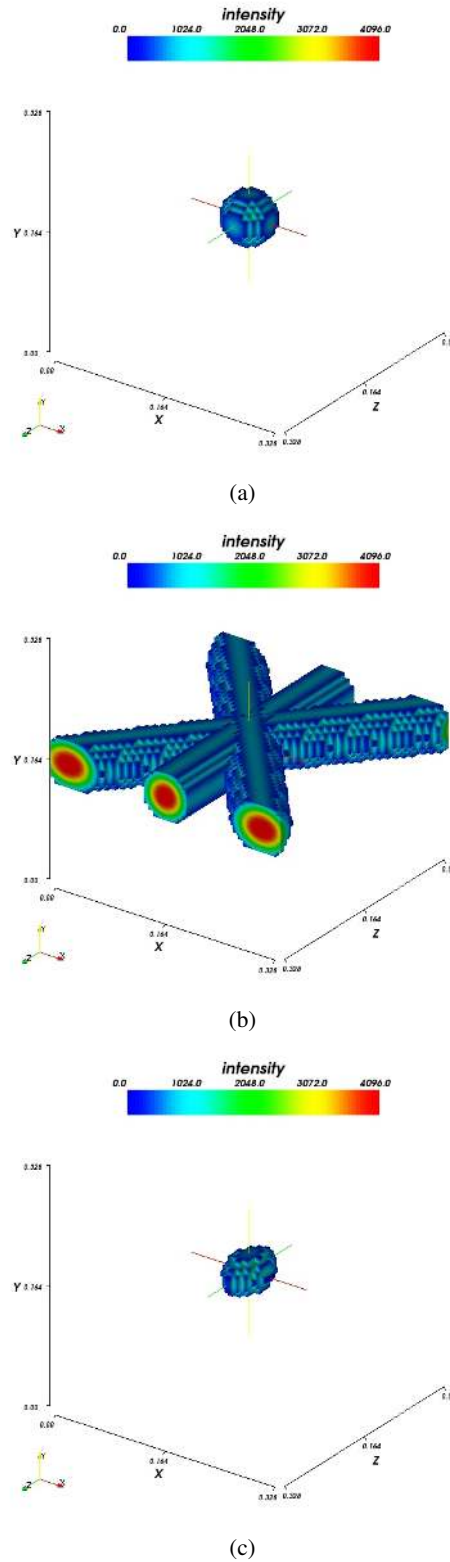

(a)

(b)

(c)

Figure 2: Multiplication of three simulated Tomo-DHPIV volume fields orientated in the same xz-plane at angular interval of 40 deg. (a) Original gaussian sphere; (b) reconstructed ellipsoids of the sphere; (c) result of ellipsoid multiplication.
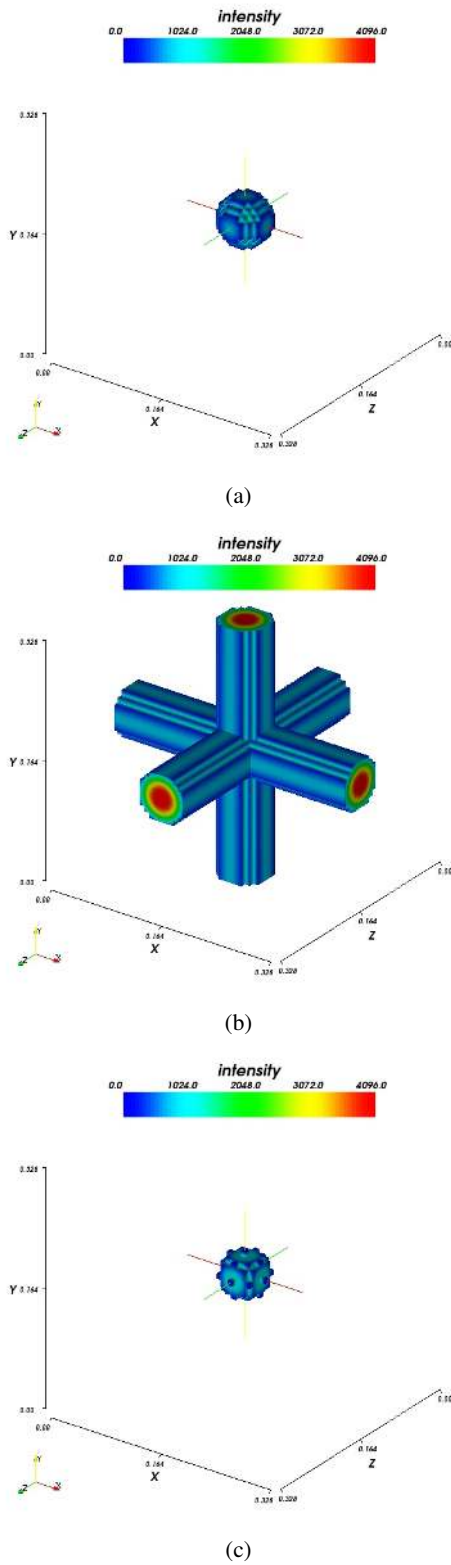
185

(a)

(b)

(c)

Figure 3: Multiplication of 3 orthogonal simulated Tomo-DHPIV volume fields. (a) Original gaussian sphere; (b) reconstructed ellipsoids of the sphere; (c) result of ellipsoid multiplication.

spacing if cross-talk between windows is to be avoided. The limitation in currently available CCD array sizes and resolution make the depth-of-field problem an inherent obstacle in DHPIV.

The Method of Tomographic DHPIV

Tomo-DHPIV or multi-camera DHPIV overcomes the depth-of-field problem via the instantaneous recording of multiple holograms of a particle seeded flow, from different viewing angles. By aligning each camera's line-of-sight with the centre of an interrogation volume and giving each camera a different orientation, the ellipsoids reconstructed from each hologram will have a unique major axis rotated about the centre of each particle. An approximation of the spherical particle can then be determined from the volume intersection of each ellipsoid. As the number of holograms increases the intersection will approach the true particle geometry in all directions, thus removing the influence of the limited depth-of-field.

The region of intersection between multiple ellipsoids can be extracted by thresh-holding and multiplying the reconstruction from each camera. This process is illustrated in figure 2, where three hologram reconstructions of a sphere are simulated at 40 deg intervals around the *y*-axis. The resulting particle closely resembles the original sphere, with a bias towards the *z*-axis resulting from the positioning of the cameras. This bias can be avoided by using orthogonal holograms (figure 3), however owing to limited optical access in many facilities this may not be possible.
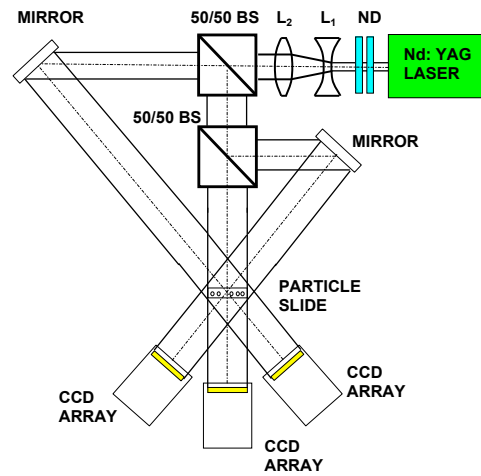

Figure 4: Schematic of Tomo-DHPIV setup.

A practical demonstration of this multi-camera holographic technique using in-line holography was been performed using a series of nominally 150 μm diameter particles situated between two glass slides. The reference and object waves were created by using an injection seeded Spectra Physics Nd:YAG laser that was expanded and separated into three beam as shown in figure 4. Holograms were recorded on 1280×1024 px PCO Pixelfly CCD arrays with a pixel size of 6.7 μm. Each hologram was reconstructed using the algorithm of Onural and Scott (5) on to $1024 \times 1024 \times 1024$ voxel 3D grid, with planes parallel to the CCD array. Each voxel grid was then interpolated on to a common grid before multiplication was applied. This interpolation is the most computationally demanding step of this technique, requiring mapping of one 3D voxel grid ($1024^3 \times 2$ btyes ≈ 2.15 GB) to another for each hologram.

The recorded holograms and reconstructions for this case can be seen in figure 5. Results show that the multiplication not

only removes the depth-of-field problem (figure 5(c)) but also removes most of the noise present in the hologram reconstruction. Following this standard cross-correlation techniques can be used to determine the 3C-3D particle displacements between Tomo-DHPIV reconstructed volume pairs.

Tomo-DHPIV Parametric Simulations

Simulation method

In order to determine the potential performance range and optimal configuration for Tomo-DHPIV, a series of Monte Carlo simulation were performed. To reduce the processing time a single 1000×1000 voxel xz-plane was considered, with each hologram given a different angular offset about the y-axis. Random particle locations were generated with a reconstruction being simulated for each hologram based on in-line holograms with effective aperture angles given by equation 7. The minor (a,b) and major (c) ellipsoid dimensions in each direction were then determined from the particle diameter and the aperture limited resolutions $\Delta_{x,y}$ and Δ_z by:

$$a = b = \frac{1}{2}\sqrt{d^2 + \Delta_{x,y}^2} \qquad (8)$$

$$c = \frac{1}{2}\sqrt{d^2 + \Delta_z^2} \qquad (9)$$

These dimension were used to determine the effective spherical radius (r) of the ellipsoid centred at (x_o,y_o, z_o), which was then used to determine intensity $I(x,y,z)$ at any given point of the ellipsoid based on a Gaussian with a peak intensity of 4096:

$$r = \frac{(x - x_o)^2}{a^2} + \frac{(y - y_o)^2}{b^2} + \frac{(z - z_o)^2}{c^2} \qquad (10)$$

$$I(x,y,z) = 4096 \exp \frac{-r^2}{0.2} \qquad (11)$$

Each ellipsoid was then mapped to the orientation of its associated hologram. All simulation parameters have been non-dimensionalised by the laser wavelength λ.

An example of such fields is given in figure 6. In 6(b) it can seen that in some cases ellipsoid from different particles will overlap. When an ellipsoid from each direction overlaps at a given point multiplication will not be able to distinguish this point from a particle and it will therefore remain as an artefact of the reconstruction process. From here on we shall refer to these artefacts as ghost particles.

The reconstructed quality of these simulation has been assessed in two ways. The first involves the correlation of the reconstructed intensity field $I_{rec,j}$ with the reference field $I_{gaus,j}$ involving Gaussian spheres located at the generated particle locations. The resulting reconstruction coefficient is given by:

$$Q = \frac{\sum_j I_{rec,j} I_{gaus,j}}{\sqrt{\sum_j I_{rec,j}^2 \sum_j I_{gaus,j}^2}} \qquad (12)$$

This coefficient indicates the overall error in the reconstructed particle field, including variation in particle locations, the presence of ghost particle, and changes in particle shape.

The second measure for comparison is the percentage of ghost particles to the true or original particles in the field. Particle were located in each reconstructed field via a basic region merging technique. This involved creating a region for each voxel above a specified threshold intensity, then merging all adjacent regions until the intensity field was divided into a series of non-connection particle regions. These region were then compared
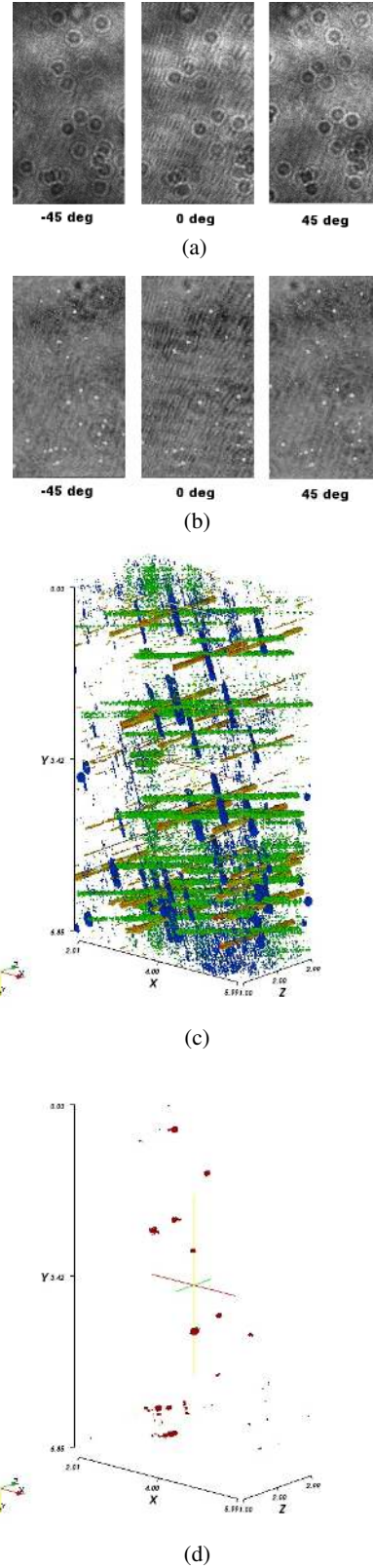

Figure 5: Tomo-DHPIV reconstruction of 150 μm particles from 3 holograms orientated in the same xz-plane at angular interval of 45 deg. (a) Recorded holograms; (b) reconstructed holograms at the normal to the holograms depth-of-field at the centre of the volume; (c) reconstructed intensity iso-contours from each hologram on the interpolated 3D voxel grid; (d) intensity iso-contours after multiplication of each each reconstructed volume.
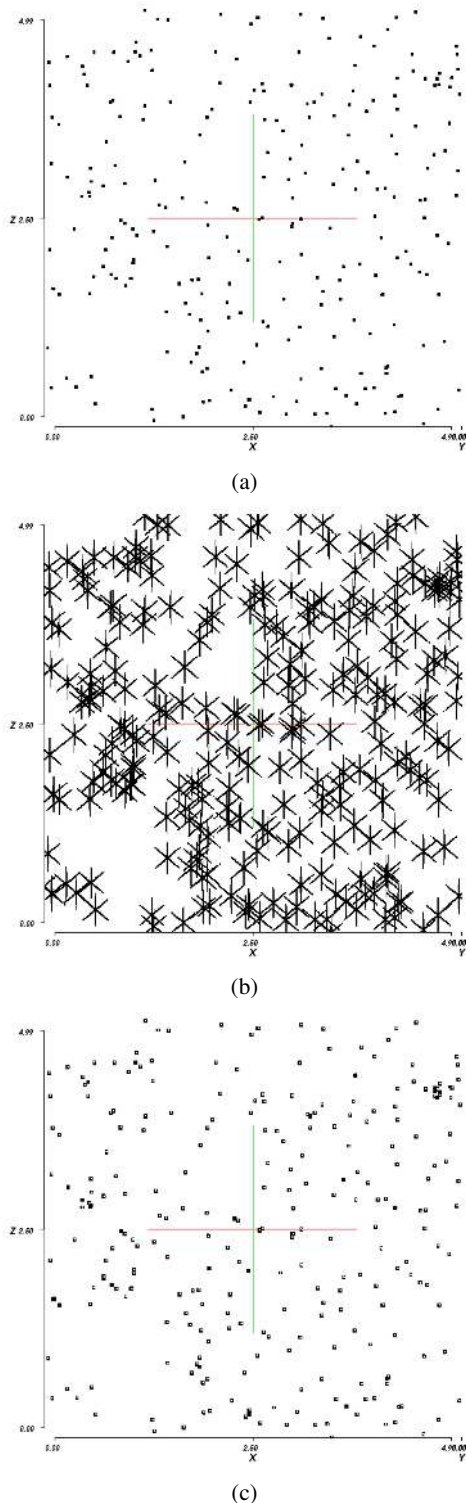
(a)

(b)

(c)

Figure 6: Simulated 1000×1000 voxel field with voxel size 9.4λ. (a) 250 original Gaussian spherical particles of diameter 28.2λ; (b) Superimposed reconstructions from three holograms orientated in the same *xz*-plane at angular interval of 50 deg; (c) result of ellipsoid multiplication hollow squares correspond to the orignal particles, solid squares represent reconstruction artefacts or ghost particles.

with the original reference field, where non-zero reference voxels in a reconstructed region indicate a true reconstructed particle.

Simulation results

Simulations consisting of 500 random fields each were performed to investigate the effects of the angular interval between holograms or cameras, the number of cameras, the particle size, and the particle number. The standard deviation of results indicated a 95% confidence interval variation in the mean correlation coefficient Q of ±0.002 and in the percentage of ghost particle $\pm2\%$.

The results of the simulation can be seen in figure 7. As should be expected the reconstruction coefficient increases as the outer two camera start to become orthogonal to each other at 45 deg and all traces of ellipsoid elongation are removed. It should also not be a surprising to see a maximum at 60 deg where the three cameras' lines-of-sight evenly divide plane into sixths. Increasing the angle however also increases the percentage of ghost particles as the intersection of ellipsoids increases. In Tomo-DPIV the consistent change in particle shape at low angular separation should not effect the velocity detections as long as the reconstructed particles do not extend across multiple interrogation regions. Ghost particles on the other-hand will generate erroneous correlation peaks and may bias a calculated vector field. For these reasons a three camera setup will probably be most effective with an angular interval around 30 deg.

As the number of cameras or instaneously recorded holograms is increased (figure 7b) the generation of ghost particles becomes negligible. This means that if 4 or more cameras can be used, then a more accurate particle shape can be returned without having to worry about an increase in ghost particles. A further point to note is that as the number of camera and multiplication operations increases, the particle intensity distribution will not increase linearly across the particle. Instead the central peak of each particle will increases faster than the edges, resulting in a fading of the edges into the background and a trimming of the particle, which should be considered if attempting to use this technique for particle or droplet sizing.

Figure 7c shows that the most dramatic influence on the performance of this reconstruction technique comes from the particle size. This follows from equations 4 and 7 where for in-line holography the size of the ellipsoid increases with the square of the particle diameter. As the particle ellipsoid elongation is increased so to is the probability of multiple ellipsoid overlap, leading to the formation of ghost particles. This simulations suggest that if particles diameter over 40λ are to be considered then it will probably be necessary to use 5 or more cameras. A similar effect is observed as the number of particles in the measurement volume increases, consequently increasing the probability of ellipsoid overlap.

As a results of the region merging algorithm for true and ghost particle identification it was also possible to determine a probability density function (PDF) for both the mean and ghost particle voxel intensities. Figure 8 shows the PDF for the reconstruction from three camera at 50 deg intervals as in figure 6. From this is can be seen that if accurate particle size is not of primary interest it should be possible to remove many of the ghost particles by simple thres-holding.
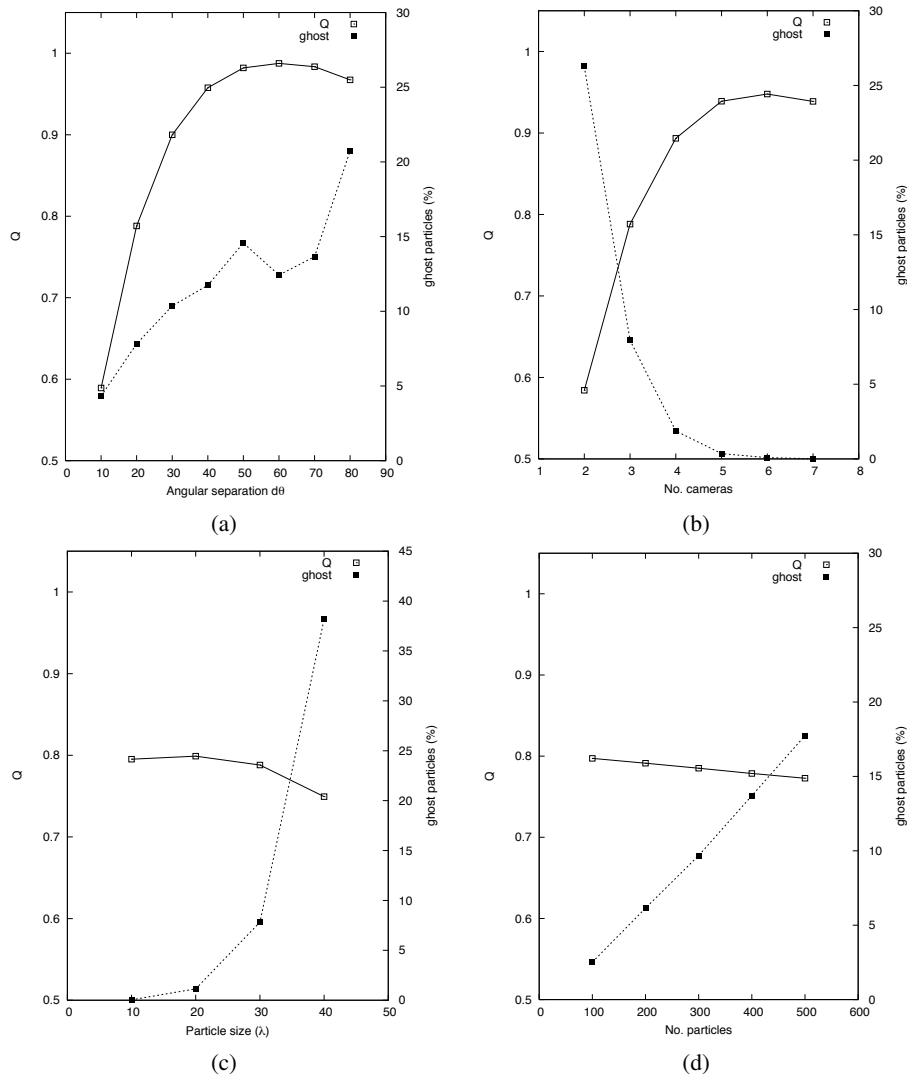
Figure 7: Reconstruction coefficient and percentage of ghost particle for Monte Carlo simulations of Tomo-DHPIV reconstruction with: (a) angular separation between three cameras or holograms; (b) number of camera or holograms with a 20 deg interval between each; (c) particle size; (d) particle number.
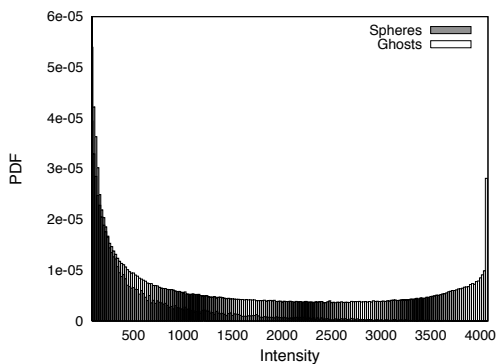

Figure 8: Probability density function of true and ghost particles

Conclusions

The technique of Tomo-DHPIV has been shown to remove the reconstructed particle elongation that is created by limited reconstruction resolution normal to a hologram. Monte Carlo simulations indicate that seeding particle densities on the order of 0.00025 particles/voxel should be obtainable using three cameras with angular separation of 30 deg, assuming cameras or CCD array with sufficient information capacity can be used.

Acknowledgements

*

References

[1] Hodkinson, J. R., Particle sizing by means of the forward scattering lobe, *Applied Optics*, **5**, 1966, 839.

[2] Keane, R. D. and Adrian, R. J., Theory of cross-correlation analysis of piv images, *Applied Scientific Research*, **49**, 1992, 191–215.

[3] Meng, H., Pan, G., Pu, Y. and Woodward, S. H., Holographic particle image velocimetry: from film to digital recording, *Measurement Science and Technology*, **15**, 2004, 673–685.

[4] Okoshi, T., *Three-dimensional imaging techniques*, Academic Press Inc., New York, 1976.

[5] Onural, L. and Scott, P. D., Digital decoding of in-line holograms, *Optical Engineering*, **26**, 1987, 1124–1132.

[6] Soria, J. and Atkinson, C., Multi-camera digital holographic imaging piv versus tomographic imaging piv - comparison and contrast of these two 3c-3d piv techniques, in *Proc. Int. Workshop on Digital Holographic Reconstruction and Optical Tomography for Engineering Applications*, editors J. Coupland and J. Lobera, Loughborough University, 2007.